Neuromorphic Artificial Touch for Categorization of Naturalistic Textures

Article *in* IEEE Transactions on Neural Networks and Learning Systems · September 2015

DOI: 10.1109/TNNLS.2015.2472477

CITATIONS
107

READS
1,234

3 authors:

Udaya Bhaskar Rongala
Lund University
19 PUBLICATIONS **593** CITATIONS
SEE PROFILE

Alberto Mazzoni
Sant'Anna School of Advanced Studies
196 PUBLICATIONS **3,869** CITATIONS
SEE PROFILE

Calogero Maria Oddo
Sant'Anna School of Advanced Studies
147 PUBLICATIONS **6,353** CITATIONS
SEE PROFILE

Neuromorphic Artificial Touch for Categorization of Naturalistic Textures

Udaya Bhaskar Rongala, Alberto Mazzoni, and Calogero Maria Oddo, *Member, IEEE*

***Abstract*— We implemented neuromorphic artificial touch and emulated the firing behavior of mechanoreceptors by injecting the raw outputs of a biomimetic tactile sensor into an Izhikevich neuronal model. Naturalistic textures were evaluated with a passive touch protocol. The resulting neuromorphic spike trains were able to classify ten naturalistic textures ranging from textiles to glass to BioSkin, with accuracy as high as 97%. Remarkably, rather than on firing rate features calculated over the stimulation window, the highest achieved decoding performance was based on the precise spike timing of the neuromorphic output as captured by Victor Purpura distance. We also systematically varied the sliding velocity and the contact force to investigate the role of sensing conditions in categorizing the stimuli via the artificial sensory system. We found that the decoding performance based on the timing of neuromorphic spike events was robust for a broad range of sensing conditions. Being able to categorize naturalistic textures in different sensing conditions, these neurorobotic results pave the way to the use of neuromorphic tactile sensors in future real-life neuroprosthetic applications.**

***Index Terms*— Neuromorphic artificial touch, neuroprosthetics, neurorobotics, spike-based decoding, tactile sensing.**

I. Introduction

A. Motivation

NEUROMORPHIC systems can emulate the spike-based neuronal mechanisms that are observed in natural effectors and senses, and thus have a potential application scenario in neurorobotics and neuroprosthetics. Specifically, neuromorphic computation is becoming an enabling technology for the development of advanced robotic systems able to interact with real-life environments.

In recent years, the implementation of neuromorphic chips has led to a drastic improvement in robots' perceptual skills [1], also because this approach can allow a lean implementation of the processing core, therefore reducing the computational and data storage burdens by means of event-based architectures [2]. For instance, custom neuromorphic circuits have proved able to mimic the dynamics of biological neurons with the desired level of detail in an energy-efficient way [3] and are particularly suited in reproducing the real-time interactions with environments [4]. Provided that proper neural interfaces will be available for upper limb neuroprostheses [5], [6], neuromorphic sensors can emulate human mechanoreceptors to target the partial restoration of natural tactile feedback, which is a major need in manipulation tasks [7]. Considering the hybrid-bionic connection between the artifact and the nervous system, the proofs of feasibility of restoration of tactile capabilities were recently provided in human amputees [8], [9]. However, the restoration of fine tactile skills, such as the categorization of textural features, is still missing. Toward this ambition, in this paper, we present a neuromorphic approach for the encoding and processing of tactile stimuli.

The quest for truly biomimetic artificial touch might also contribute to the open scientific debate about the neuronal mechanisms underlying the human sense of touch. The firing dynamics of fingertip mechanoreceptors during manipulation tasks has been extensively studied over the past decades [10]–[14]. Recent neuroscientific investigations were able to map the representation of tactile input features up to the cuneate nucleus [15], the thalamus [16], and the primary somatosensory cortex [17], [18]. However, a unifying understanding of touch perception from periphery to cortical areas is missing, and the integrated modeling is still hypothetical [19]. The investigation of neuromorphic encoding might help evaluating different candidate mechanisms for tactile information transduction and processing.

The development of a realistic spiking mechanoreceptor and overall architecture still needs to be consolidated, and thus in this paper, we do not proceed directly to the artificial neuromorphic implementation in hardware. Rather, we undertake a soft neuromorphic approach [20] through the Izhikevich model [21], to be able to tune the neuron firing parameters. This is a preparatory step toward the future hardwired implementation of the mechanoneurotransduction processes.

B. State of the Art and Related Work

Several tactile sensing technologies were inspired by the morphology of the biological tactile system [22], [23]. Recent trends in artificial touch include biohybrid sensing on the

Manuscript received November 14, 2014; revised August 17, 2015; accepted August 22, 2015. This work was supported in part by DG Connect through the NEBIAS European Project entitled NEurocontrolled BIdirectional Artificial Upper Limb and Hand Prosthesis under Grant EU-FP7-ICT-611687, in part by the Italian Ministry of Foreign Affairs and International Cooperation through the Directorate General for Country Promotion (Economy, Culture and Science)–Unit for Scientific and Technological Cooperation via the SensBrain Italy–Sweden Bilateral Research Project entitled Brain Network Mechanisms for Integration of Natural Tactile Input Patterns, in part by the Ministero dell'Istruzione, dell'Università e della Ricerca (MIUR) through the Italian Progetti di Rilevante Interesse Nazionale (PRIN) programme with the HandBot Project entitled Biomechatronic Hand Prostheses Endowed with Bio-Inspired Tactile Perception, Bi-Directional Neural Interfaces and Distributed Sensori-Motor Control under Grant CUP: B81J12002680008 prot.: 20102YF2RY, and in part by the European Commission through the NanoBioTouch European Project entitled Nanoresolved Multiscale Investigations of Human Tactile Sensations and Tissue Engineered Nanobiosensors under Grant EU-FP7-NMP-228844.

The authors are with the Scuola Superiore Sant'Anna, The BioRobotics Institute, Pontedera I-56025, Italy (e-mail: u.rongala@sssup.it; a.mazzoni@sssup.it; oddoc@sssup.it).

Color versions of one or more of the figures in this paper are available online at http://ieeexplore.ieee.org.

Digital Object Identifier 10.1109/TNNLS.2015.2472477

physical perspective [24]–[26] and the use of Bayesian filters for tactile classification of large sets of naturalistic stimuli as the processing methodology based on synthetic sensor outputs [27]. Elegant studies presented direct and inverse functions describing tactile interaction [28], [29], investigated the role of fingerprints [30], and combined the modeling of slip mechanics and the experimental identification of the event with various textures and interaction conditions [31].

Such prior studies grounding on consolidated transduction principles did not emulate the spiking code of tactile information that is observed in biological mechanoreceptors. This is, instead, addressed by the few neuromorphic tactile sensing applications that have been developed so far. A piezoresistive sensor inspired by cricket cerci was coupled with a neuromorphic chip implementing the behavior of adaptive integrate and fire neurons [32], [33]. A robot able to actively explore the surrounding environment with tactile sensors was developed by reproducing the biological details of the rat's whisking behavior from the modeling and physical implementation of the whisker [34], [35], to the primary afferent neurons, to the midbrain tactile information processing [36]–[38].

To the best of our knowledge, just a limited number of groups so far addressed the neuromorphic artificial development of glabrous fingerpad mechanoreceptors using neural spikes to represent sensor outputs, as briefly discussed in the following. Kim *et al.* [39] reproduced spike timing in mechanoreceptive fibers during manipulation tasks with integrate-and-fire neuron models. Bologna *et al.* [40], [41] injected the output of a force sensor in a leaky integrate-and-fire model of slowly adapting mechanoreceptors to study how the resulting spike trains encoded the Braille stimulation. Spigler *et al.* [20] followed by Lee *et al.* [42] coupled sensors with the Izhikevich models of adapting neurons to investigate how the spike trains output were modulated by surface properties. The same Izhikevich spiking model was translated into a subsequent wearable application addressing gait segmentation via shoes endowed with pressure sensors [43]. Finally, Kim *et al.* [44] developed spiking artificial tactile sensors, in parallel to a comprehensive modeling of the firing dynamics of slowly adapting mechanoreceptors [45], which were successfully applied for peripheral neural stimulation in animal studies [46].

C. Contribution

In preparation of future neuroprosthetic and neurorobotic applications, we further explored the trend of neuromorphic sensors, and here, we present results showing that spike trains were able to classify real-life textures. Moreover, for the first time to the best of our knowledge, we challenged the classifier by systematically evaluating a broad range of tactile stimulation conditions. Specifically, we assessed the artificial neuromorphic encoding of ten daily life textures under 25 combinations of sliding velocity and contact force conditions, with ten repetitions per stimulus, therefore yielding to a total number of 2500 experimental sessions. We demonstrated that the implemented categorization of naturalistic textures was robust to the variations of sliding velocities, and we settled the foundations in order to account for force variations in future studies.

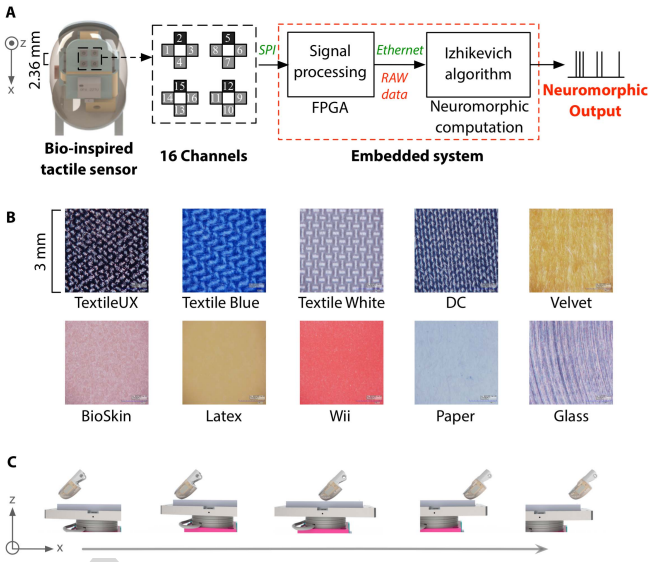

Fig. 1. (A) Sensor data processing. From left to right: illustrative representation of the fingertip structure on the top of which the bioinspired tactile sensor is placed, and a spatial arrangement of the 16 channels. Sensor outputs are sampled via ADC (ADS1258, Texas Instruments, USA) and conveyed to the embedded FPGA system through a serial peripheral interface, where the raw sensor data are preprocessed and then relayed through Ethernet to a PC. Here, the raw data are fed into the Izhikevich neuronal models mimicking the dynamics of adaptive mechanoreceptors. (B) Microscopy images (KH-7700 Digital Optical Microscope, Hirox Corp., Japan) of the tactile stimuli that are presented to the sensors. Top row: five textiles. Bottom row: five nontextiles. Each picture shows a 3-mm $\times$ 3-mm square patch of the stimulus. Note that the lines in the glass appear in transparency from the surface below, whereas glass surface is quite smooth. (C) Trajectory path of passive touch protocol. From left to right: preparation, normal indentation (z-axis) before sliding (x-axis), tangential sliding, indentation after sliding, and retraction.

Overall, in this paper, we demonstrated that our neuromorphic system is able to encode naturalistic textures under different sensing conditions and might therefore be suited for tactile information processing in real-life applications.

II. Materials and Methods

A. Artificial Finger and Experimental Platform

The core element was a Micro Electro-Mechanical System (MEMS) sensor (1.5 mm $\times$ 1.5 mm $\times$ 625 μm) fabricated through silicon micromachining technologies [47]. Each sensor had four piezoresistors implanted at the roots of a cross shape, with a mesa-structure in its center acting as a force catalyst toward the transducers. According to the sensor physical features, the four piezoresistors show a homogeneous response magnitude and sign to normal forces. Conversely, the tangential components along a tether pair of the cross elicit marked responses, with alternate sign, on the two piezoresistors implanted on the direction of such tethers, and almost null responses on the two piezoresistors implanted on the orthogonal tethers [48]. The bioinspired fingertip used in the experiments integrated a 2 $\times$ 2 array of such MEMS sensors [49] [Fig. 1(A)], with a 2.36-mm pitch. Therefore, the total number of channels was 16 in a 22.3-mm^2 area (0.72 transducers/mm^2) mimicking the density of Merkel slowly adapting type I human

mechanoreceptors in the palmar side of the fingers [11]. Sensor outputs were sampled at 380 Hz by means of an analog-to-digital converter (ADC) (ADS1258, Texas Instruments, USA) integrated over a rigid-flex printed circuit board, which was lodged on a human-sized distal phalanx and covered with a compliant polymeric material (DragonSkin 10, Smooth-on, USA) [50]. The stimuli [Fig. 1(B)] were indented and slid through a mechatronic platform [51] having two orthogonal degrees of freedom [Fig. 1(C)]. The platform is in parallel being used for psychophysical and electrophysiological human-touch studies, and in this paper, it was applied to indent and slide the tactile stimuli tangentially to the artificial fingertip. A normal contact force and the sliding velocities were feedback controlled, and were recorded synchronously with the outputs of the artificial biomimetic sensors and neuromorphic spike trains.

B. Stimuli

We selected ten different naturalistic tactile stimuli in this experimentation, out of which five were textile and five were nontextile stimuli [Fig. 1(B)]. The selected textiles were low friction materials and had a patterned distribution of crests along the surface, whereas the nontextile stimuli had a broad spectrum of physical properties. BioSkin is an artificial skin-like material with medium friction and distributed patches with irregular surface. Latex and glass are high-friction materials with a grain size as low as 90 nm, distributed across the surface. Wii (cover of Nintendo Wii console) has an extrafine surface with very low friction.

C. Experimental Protocol

The capability of the developed neuromorphic sensory system to characterize the stimuli was evaluated under a passive touch protocol [52] [Figs. 1(C) and 2]: the fingertip was fixed and the stimulus was slid by means of the mechatronic platform, in order to elicit a relative motion at the interface between the artificial finger and the stimulus. At first, the stimulus was located ∼50 mm below the fingertip (preparation phase). Then, it was raised until it reached the desired contact force with the sensor (indentation phase, z-axis). After 4 s, while keeping the contact force regulated, the stimulus was slid for 60 mm with a fixed sliding velocity (sliding phase, x-axis, always from the same starting x-position). Subsequently, the movement stopped, and the fingertip was held still for 1 s in contact mode (indentation after sliding phase). Finally, the stimulus was retracted to the initial position (retraction phase). This procedure was repeated ten times for each stimulus.

In order to study the relation between neuromorphic texture encoding and sensing dynamics, the contact force was modulated between 200 and 600 mN with a step of 100 mN, and the sliding velocity between 5 and 25 mm/s with a step of 5 mm/s for a total of 25 experimental combinations.

D. Neuronal Model and Parameters Definition

Sensor outputs were preprocessed to provide polarized input to the artificial neuron. We normalized the sensor output

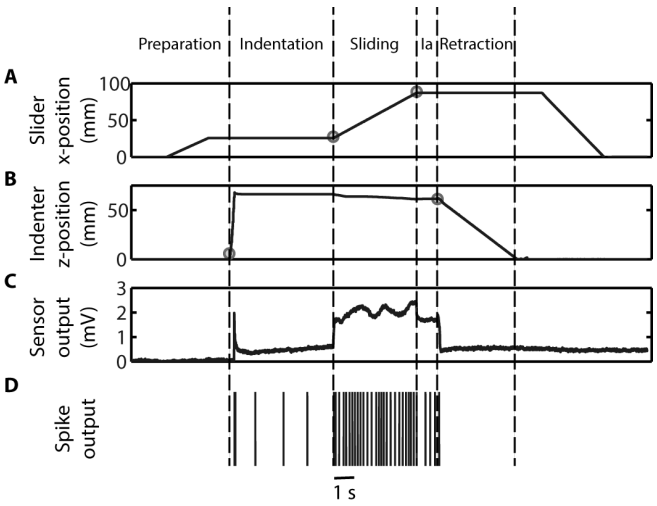

Fig. 2. Neuromorphic sensor responses for the protocol phases, with a contact force of 400 mN and a sliding velocity of 15 mm/s. Vertical dashed lines separate the five phases of protocol indicated in Fig. 1(C): preparation, indentation, sliding, indentation after sliding (Ia), and retraction. The rows illustrate different variables of the system during the protocol. (A) Finger trajectory along the horizontal axis (along the tactile stimulus). (B) Finger trajectory along the vertical axis (perpendicular to the surface of the tactile stimulus), resulting from the force-controlled indentation. (C) Raw sensor output for one representative channel used as input for the neuronal models. (D) Spike occurrences from artificial mechanoreceptor.

based on the difference between individual opponent channels data [20], [48] to focus on the shear forces arising at stimulus–finger interface as a result of the tangential sliding motion, exploiting the directional selectivity of coupled sensor outputs, as discussed in Section II-A. The outcome voltage was then multiplied by a gain factor (GF) and injected as the input current I_{input} to an Izhikevich neuron model [21]. We investigated the interspike interval (ISI) distribution of the neuron model in response to stimuli with GF between 5000 and 30 000/Ω to identify an appropriate value of this parameter (Fig. 3). Increasing the GF led to a monotonic decrease in the ISI (increase in firing rate) but also to the increase in the overlapping of the ISI distributions associated with different stimuli, indicating a lower diversity among response spike patterns. On the other hand, the low firing rate associated with a GF of 5000/Ω or less might lead to encoding problems due to: 1) a longer latency in the response affecting future real-time applications and 2) a reduced set of possible responses on short timescales. Therefore, a GF of 10 000/Ω was selected for this paper.

The Izhikevich model was chosen in order to reproduce adaptation dynamics, that is a characteristics of mechanoreceptors [19]. According to the model, the membrane potential v and the adaptation variable u were updated through the following nonlinear differential equations discretized using Euler's method:

$$\dot{v} = Av^2 + Bv + C - u + \frac{I_{\text{input}}}{C_m} \tag{1}$$

$$\dot{u} = a(bv - u). \tag{2}$$

When the membrane potential reached the spike threshold of 30 mV, one spike was produced, followed by the following

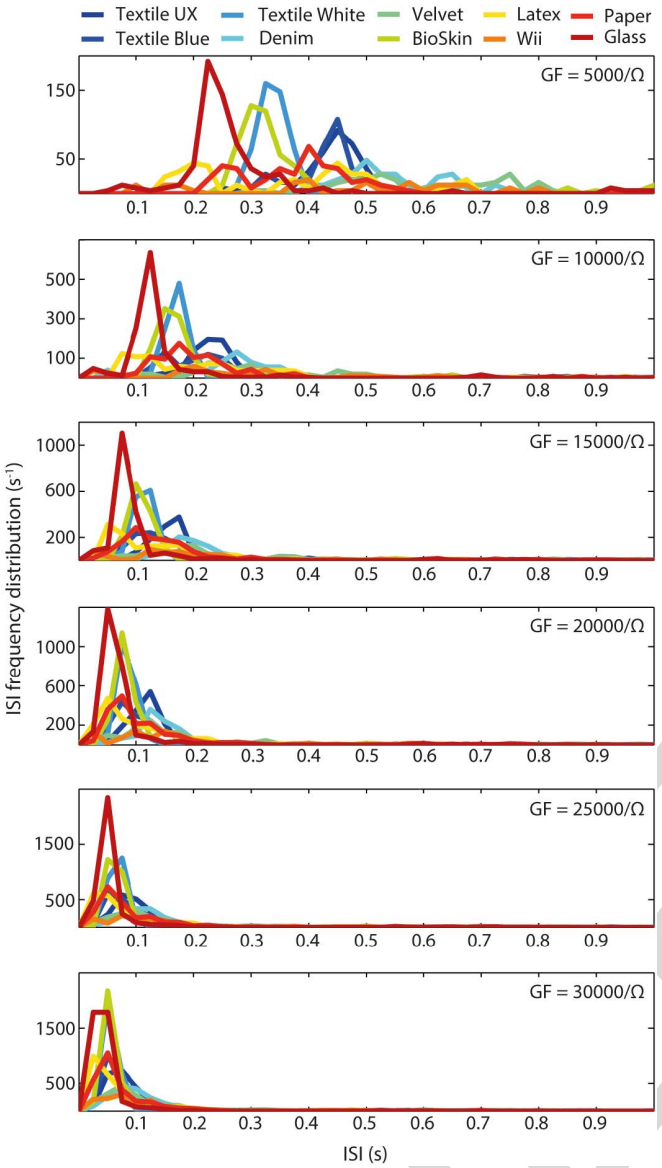

Fig. 3. Effect of GF (which converts raw sensor voltage outputs into current inputs for the Izhikevich neuron) on the distribution of the ISI. The plot shows the experimental data gathered during the 60-mm sliding phase of each of the ten stimuli, with 400-mN force and 15-mm/s velocity, and averaging over the ten repetitions of each stimulus.

after-spike resetting:

$$\text{if } v \geq 30 \text{ mV}, \quad \text{then} \begin{cases} v \leftarrow c \\ u \leftarrow u + d. \end{cases} \tag{3}$$

The A, B, C, and the spiking threshold are the standard parameters of the Izhikevich artificial neuron model, whereas the a, b, c, and d parameters were selected (Table I) so as to allow a regular spiking behavior [21], [53], being able to encode both sustained indentation and dynamic stimulus sliding (Fig. 2) [11].

E. Decoding Procedures

The identity of the tactile stimuli was decoded starting from the features of the spike trains emitted by single channels during the sliding phase of the experimental protocol.

TABLE I
IZHIKEVICH MODEL PARAMETERS USED IN THE EXPERIMENTAL EVALUATION OF THE NEUROMORPHIC SENSOR

A	B	C	C_m	a	b	c	d
0.04 $s^{-1}V^{-1}$	5 s^{-1}	140 Vs^{-1}	1 F	0.02 s^{-1}	0.2	-65 mV	8 mV

We performed the first classification by means of two features: the average spike rate during the sliding phase combined with the coefficient of variation (CV) of the ISI during the same phase, defined as

$$\text{ISI}(\text{spike}_n) = t(\text{spike}_n) - t(\text{spike}_{n-1}) \tag{4}$$

$$\text{ISI CV} = \frac{\text{std}(\text{ISI})_{\text{spikes}}}{\langle \text{ISI} \rangle_{\text{spikes}}}. \tag{5}$$

The first decoding evaluation was performed over this 2-D space of responses using a k-nearest neighbors (knn) algorithm with leave-one-out validation and Euclidean distance [54].

In the second set of analyses, we pursued an approach based on precise spike timing [55], and to this aim, we measured the distance between the spike trains in each pair of trials by means of Victor Purpura distance (VPd) [56]. Briefly, the metrics measure the cost of transforming one spike train into another by the following two operations: 1) adding/removing a spike (cost: 1) and 2) shifting the time of a single spike by an interval Δt (cost: $q\Delta t$, where q is a tunable parameter). The minimum cost of transforming one spike train into another is the distance between them. A short distance corresponds to similar spike trains. For each combination of stimulation parameters (force, velocity), we computed the distance between each pair of trials over all ten presentations of the ten stimuli. We classified the responses with leave-one-out validation according to the identity of the knn of each response. Finally, spike trains obtained with different sliding velocities were classified by converting the spike times in spike positions (similar to spatial event plots [18]) and repeating the procedure described above with a space shifting cost $q\Delta x$. Note that in this last evaluation, we are decoding a set of 5 velocities × 10 stimuli × 10 presentations (force was held fixed, and results with 400 mN are shown).

III. RESULTS

A. Texture Decoding

Channels 2, 5, 12, and 15 were all sensitive to the tangential force arising along the stimulus sliding direction, and we will refer to them as active channels (Fig. 4). The other 12 channels fired only sporadically because of their different directional preferences. The active channels sensed the space-shifted parts of the stimulus (either along or across the sliding direction) and fired in a pairwise similar manner (2 with 15 and 5 with 12, see Fig. 4) due to their placement on the finger surface [Fig. 1(A)]. In the following analyses, we will display results obtained from channel 2 responses that achieved an intermediate decoding performance between channel 5 and 15 (higher performance) and channel 12 (lower performance).

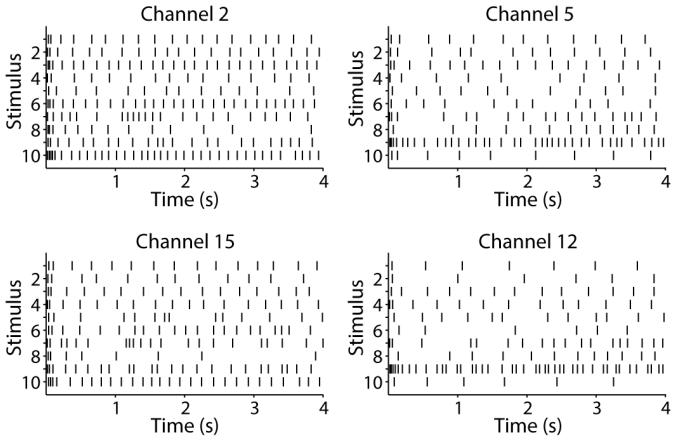

Fig. 4. Adaptive mechanoreceptor responses for all the four active channels (2, 5, 12, and 15) along the sliding direction. Each row shows the response of an artificial receptor for different tactile stimuli, for a fixed force of 400 mN and sliding velocity of 15 mm/s. The stimulus order is the same as shown in Figs. 1(B) and 5.

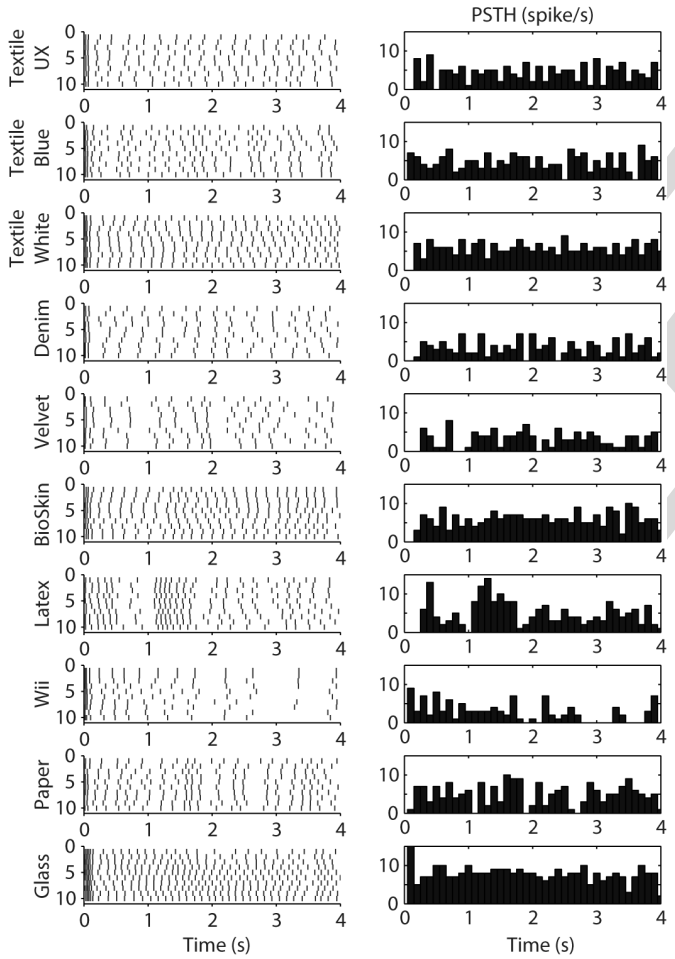

Fig. 5. Adaptive mechanoreceptor response to different tactile stimuli. Each row shows the response of an artificial receptor to a given tactile stimulus, for fixed force of 400 mN and sliding velocity of 15 mm/s. Left column: raster plot of the spiking response to each of the ten presentations of the stimulus. Right column: PSTH with 100-ms bin. This plot and all the following figures consider the activity of the same artificial mechanoreceptor, injected with an input variable resulting from channel 2 of the sensor array (see Fig. 1).

The response of the neuronal model coherently modulated across the different protocol phases: the onset of the indentation elicited a quasi-constant low rate of firing, and when the

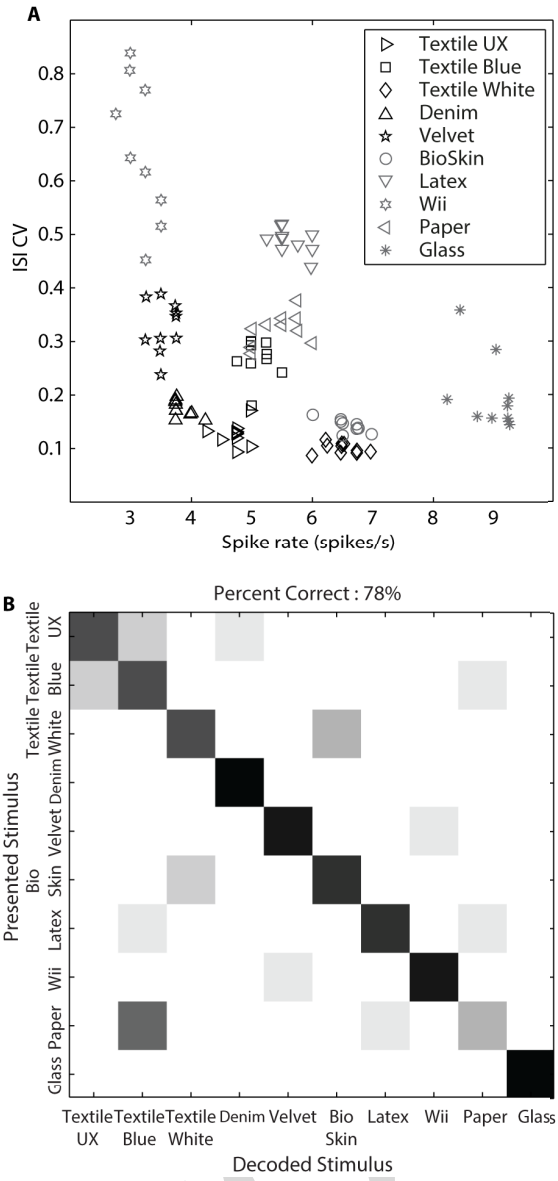

Fig. 6. Decoding based on basic spike train features. (A) Combination of spike rate of adaptive mechanoreceptor during sliding phase and CV of ISIs over the same period of time for all ten presentations of each stimulus experimented with 400-mN contact force and 15-mm/s sliding velocity. The legend indicates the marker associated with each stimulus. Note that for Wii stimulus, two repetitions appear perfectly overlapped (2^{nd} marker from the top). (B) Confusion matrix of stimulus decoding with the knn clustering algorithm applied on the aforementioned spike train features. Arrow: chance level.

stimulus was smoothly sliding, the artificial mechanoreceptors fired with almost stable rate [see Fig. 2(D) for an example pattern]. The firing rate of these artificial mechanoreceptors was roughly proportional to a raw sensor output (Fig. 2), and the temporal structure of the spikes during the sliding motion appeared to encode the stimulus identity (Fig. 5). Particularly, responses were quite reliable across the ten presentations for each of the stimuli (Fig. 5, raster plots on the left). We found that on average different stimuli elicited responses with differences in both firing rate and firing patterns [Fig. 5, poststimulus time histogram (PSTH) on the right]. Overall, textile stimuli (top five rows) triggered much more

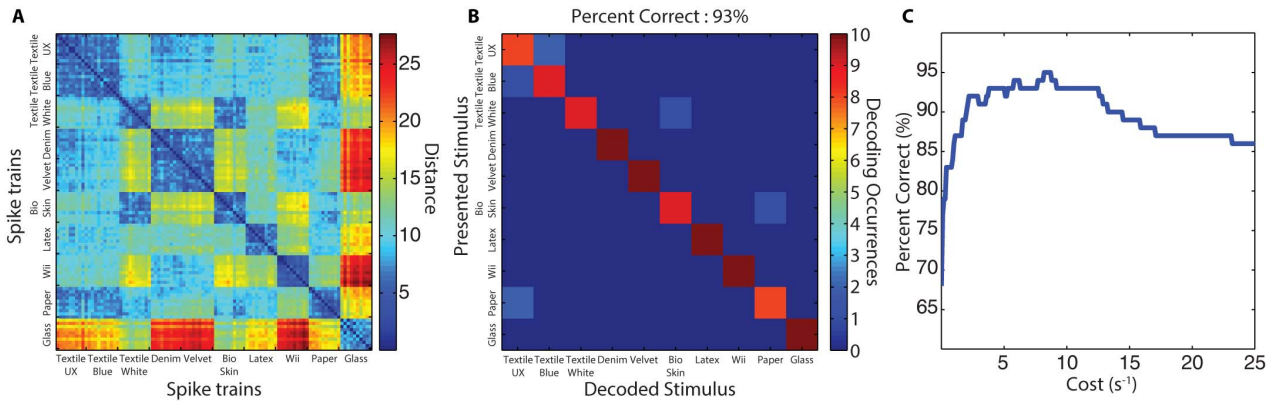

Fig. 7. Stimulus decoding based on VPd between neuromorphic sensor responses. Sensing conditions: 400-mN contact force and 15-mm/s sliding velocity. (A) VPd between every spike trains pair over all presentations of all stimuli. Spike trains are arranged in blocks of ten presentations for each stimulus as indicated by the axis labels. The cost (q) is set at 5/s. (B) Confusion matrix of stimulus decoding with the knn clustering algorithms applied on the VPd of response pair shown in (A). (C) Percent of correct stimulus decoding for different cost parameters (q) of VPd.

regular firing rates than nontextile stimuli, coherently with the fact that textile surfaces display evident spatial recurrent patterns, while nontextile surface have a finer structure [Fig. 1(B)]. Moreover, a modulation of average spike rate is observed, as a function of the identity of some of the stimuli [Fig. 6(A)]. On the other hand, also spike patterns associated with different nontextile stimuli were remarkably different as a consequence of their physical properties; the low friction Wii stimulus elicited a sparse and patterned response, while the high friction glass elicited a uniform and intense response, with paper displaying a somewhat intermediate behavior.

Considering the second dimension of the calculated features, indicatively low ISI CV was induced by regular textures, such as the ones found in textile stimuli, while the extra fine surface of stimulus Wii induced irregular slipping, and therefore was associated with a high ISI CV with large interpresentation differences. The combination of these two spike train features was sufficient to obtain a first clustering of the responses according to the characteristics of the interaction between the sensor and each stimulus [Fig. 6(A)]. We then applied a knn decoding algorithm with leave-one-out validation to the 2-D space of these responses. For sensor channel 2, optimal classification [78%, Fig. 6(B), chance level being 10%] was achieved for $k = 3$, and a coherent value was obtained when considering 1 neighbor (78% decoding) or 5 neighbors (77% decoding) showing that the results were robust to the choice of this parameter. Channels 5 and 15 achieved 93% and 92% performance, respectively, while channel 12 achieved a 68% performance.

With the aim to achieve a higher identification rate, we adopted a decoding procedure making full use of the temporal complexity of spike patterns. We measured the VPd [56] between each pair of spike train responses across all presentations of all stimuli. We found that indeed spike train responses associated with different presentations of the same stimulus were much closer (in VPd terms) than spike train responses induced by different stimuli [Fig. 7(A)]. We made use of this result to build the second knn decoding algorithm with leave-one-out validation, this time, finding the neighbors by means of the VPd metrics. This, for channel 2, resulted in a striking increase in performance to 93% (+15%) [Fig. 7(B)] for a shifting cost $q = 5$/s, indicating that the timing of spikes carried information that was not captured by spike rate and ISI CV. All active channels saw an increase in performance; when using VPd, correct decoding rose to 97% (+4%), 93% (+25%), and 96% (+4%) for channels 5, 12, and 15, respectively. We also investigated the decoding performance, as a function of the shifting cost parameter of VPd [Fig. 7(C)], and we found a decoding performance plateau between $q = 5$/s and $q = 12$/s indicating that the relevant timescale for decoding was in the 100–200-ms range. Coherently with previous results, the decoding performance for $q = 0$ (corresponding to a rate code) was 68% of correct decoding, less than the 78% performance with the combination of spike rate and ISI CV shown in Fig. 6(B).

B. Effect of Sensing Dynamics on Decoding

All results shown above were obtained with a contact force of 400 mN and a sliding velocity of 15 mm/s. In the following, we show the results with 25 combinations of force and velocity parameters to evaluate how sensing conditions affected the neuromorphic sensor response and hence the decoding. The spike rate increased with both contact force and sliding velocity (linear correlation $R > 0.9$ for both features for all textures), with a similar modulation across all textures (Fig. 8). The ISI CV, instead, was relatively insensitive to sensing dynamics.

Crucially, changes in the sensing conditions induced variations in the firing patterns that still allowed appreciating textures identity. The reason lies in the fact that spike trains are mainly reflecting the spatial structure of the texture. From this, we observe that changing the sliding velocity of a fixed texture resulted in a coherent spike train structure occurring over different time scales (hence the higher firing rate for faster sliding, Fig. 8). On the other hand, an increase in the force amplified the raw sensor signal that fed the Izhikevich neuron model, increasing the firing rate (Fig. 8). In this way,

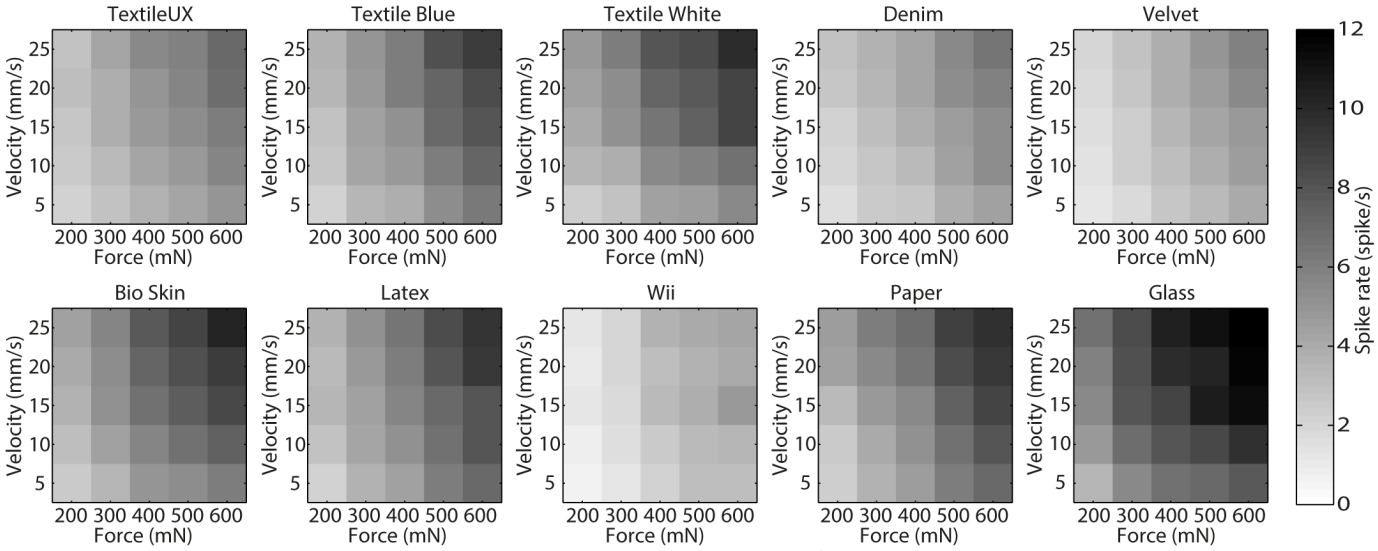

Fig. 8. Effect of sensing dynamics on spike rate. Each panel shows the firing rate elicited by a given stimulus under different sensing conditions as identified by combination of sliding velocity and contact force.

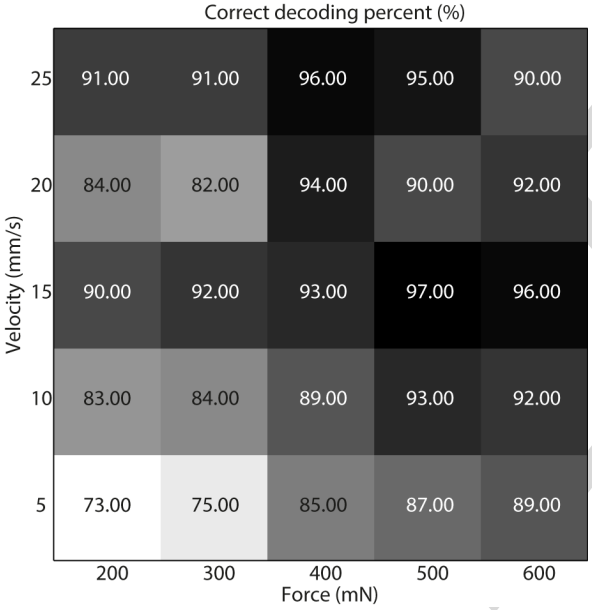

Fig. 9. Correct VPd decoding percentage across, for each tested combination of contact force and sliding velocity. Chance level is 10%. The decoding algorithm used in here is the same as that of Fig. 7.

differences in spike train structures were preserved across sensing conditions. This is proved by the fact that repeating the same VPd-based textures decoding procedure adopted above for the spike train responses elicited under different stimulation conditions led to very accurate decoding, with an accuracy higher than 90% in 15 out of 25 experimental conditions (Fig. 9). A lower performance was associated with the combination of slow sliding velocity (5 mm/s) and weak contact force (200 mN), probably due to the very low firing rate elicited and stick-slip sliding regime, but still yielded a 73% of correct decoding over 10% chance level.

We noticed that the patterns of the spike trains elicited by the same stimulus and contact force at different sliding

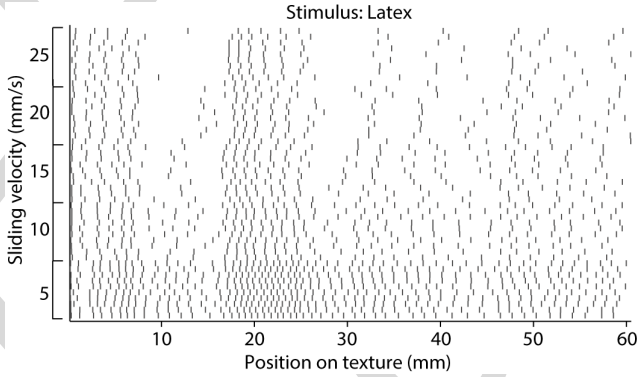

Fig. 10. Spike trains scaled according to the fingertip position relatively to the texture in response to representative tactile stimulus for all sliding velocities (5, 10, 15, 20, and 25 mm/s) and for a fixed force (400 mN). All ten repetitions of stimulus presentation are displayed for each sliding velocity.

velocities were similar when rescaled according to the velocity (spatial event plots, Fig. 10). This is coherent with the fact that artificial mechanoreceptor spike trains are transducing the spatial structure of the texture, and it supports the possibility of having a general decoding procedure across different sliding velocities.

We devised such a procedure defining a spatial VPd (sVPd): after the rescaling of the spike times according to the sliding velocity, we determined the sVPd replacing the classic time-shifting cost with a space-shifting cost (see Section II-E for details). As an example for a fixed force of 400 mN, Fig. 11(A) shows the computed sVPd between all spike trains elicited by all stimuli for all sliding velocities (5, 10, 15, 20, and 25 mm/s). The higher distances systematically shown for 5 mm/s are due to a stick-slip regime of stimulus-finger contact at such low velocity.

Then, we categorized the textures independently of the sliding velocity with the same knn decoding algorithm with leave-one-out validation used in Section III-A on this new space of distances. We achieved a high value of 90% of correct

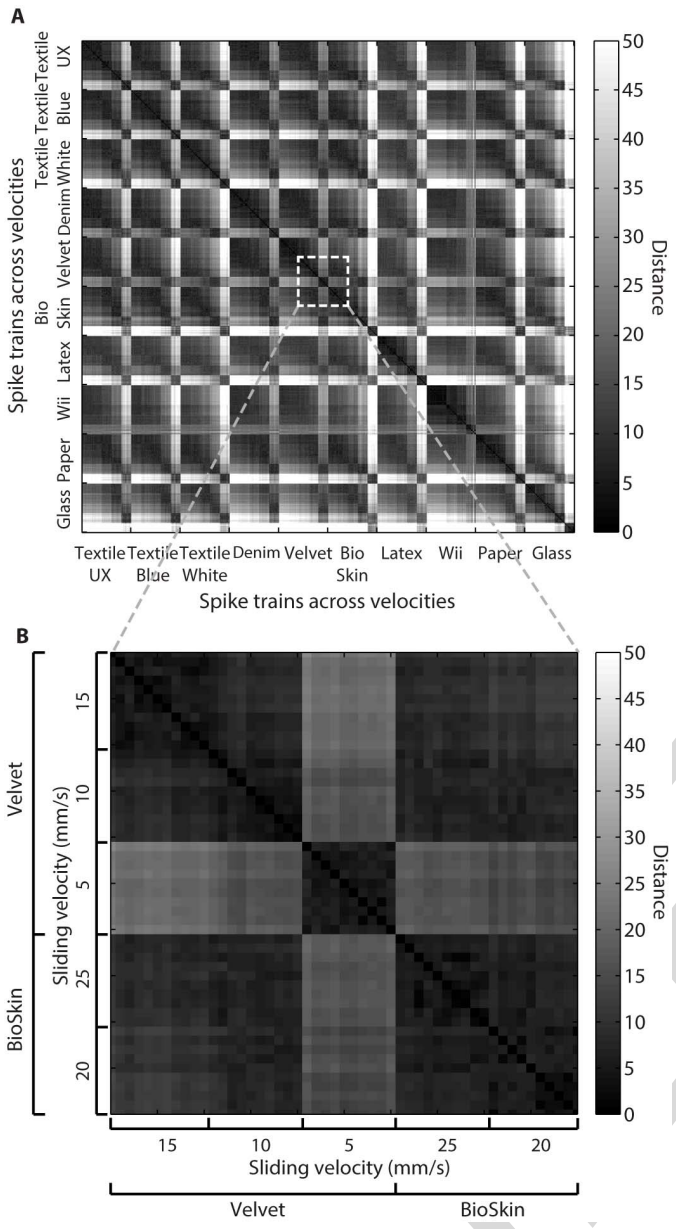

Fig. 11. Stimulus decoding based on sVPd between responses along all inspected sliding velocities. (A) sVPd between every spike train pair over all presentations of all stimuli for all five experimented sliding velocities. Spike trains are arranged in blocks of 50 presentations for each stimulus (ten presentations for each of five sliding velocities ranging from 5 to 25 mm/s), as indicated by the axes labels. The sVPd cost is set to 0.3/mm. (B) Close-up view of a region of (A) showing how velocity modulates in building the matrix.

decoding over 500 presentations (10 textures, 5 velocities, 10 repetitions each, fixed 400-mN force), with most of the misclassification within textiles (Fig. 12). However, it was not possible to apply a similar rescaling to build a VPd-based decoding mechanism working across different contact forces. We evaluated then whether it was possible to decode the textures normalizing the spike rate dividing it for the contact force and combining it with the ISI CV, similar to the approach shown in Fig. 6. We found that the decoding performance in this case was 48%, above chance level, but far from the results obtained for decoding across sliding velocities.

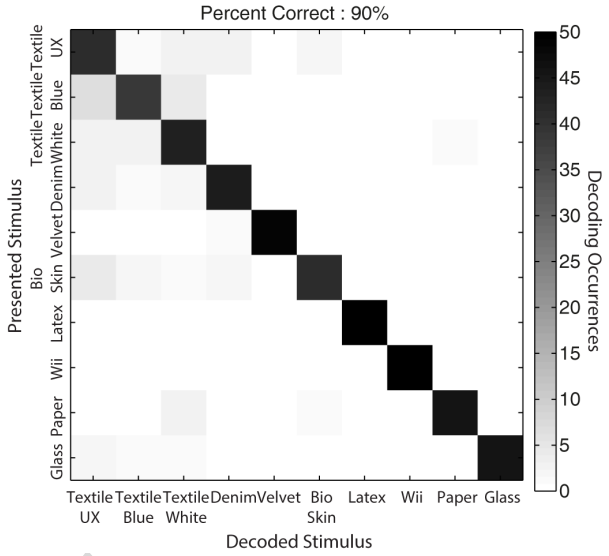

Fig. 12. Confusion matrix of stimulus decoding with the knn clustering algorithms applied on the sVPd of response pair over all presentations of all stimuli for all five inspected sliding velocities.

IV. Conclusion and Discussion

A. Main Achievements

We developed a neuromorphic artificial tactile system by injecting the output of a bioinspired tactile sensor into adaptive neuronal models producing spike trains [Fig. 1(A)].

We investigated whether spike trains elicited by the contact with different naturalistic textures [Fig. 1(B)] were sufficiently diverse and reliable to allow for decoding the presented stimuli. During the sliding phase [Fig. 1(C)], our artificial mechanoreceptor model produced spike trains that reflected the spatial structure of the inspected textures (Fig. 5), and were consequently used for stimuli decoding. We investigated the classification properties of different features of the receptor response. The combination of the spike rate with the regularity of the spike trains as evaluated by the ISI CV was sufficient to decode the experimented stimuli with an accuracy between 68% and 93% depending on the sensor channel (see Fig. 6 and Section II-A).

In the second set of analyses, we decoded the responses according to the VPd between spike trains. This led to a sharp improvement of decoding (see Fig. 7 for 400 mN and 15 mm/s), with lower variability among active channels (for 400 mN and 15 mm/s stimulation conditions, 93% worst case decoding with channels 2 and 12 and 97% best case with channel 5) indicating that the differences in the precise timing of spikes carry information about the inspected stimuli that is not present in the spike rate average and variation coefficient. The major role of precise spike timing is also consistent with recent neuroscientific findings [15], [19], [55], [57]. The future experimental protocols involving a peripheral neural stimulation of amputees may be explanatory in this respect.

In this paper (Section III-B), we investigated the effect of changing sliding velocity and contact force in the receptor response and hence in the decoding accuracy. The variation of force and velocity stimulation parameters resulted in activity modulations that were highly homogenous across textures (Fig. 8). Consequently, we showed a decoding

TABLE II
STORAGE REQUIREMENT FOR BOTH RAW (SHADED REGION) AND NEUROMORPHIC SENSOR DATA GATHERED ALONG THE SLIDING PHASE (60 mm) FOR EACH STIMULATION CONDITION, FOR A SINGLE CHANNEL SENSOR DATA

		Force (mN)				
		200	300	400	500	600
Velocity (mm/s)	25	3.6 kB	3.6 kB	3.6 kB	3.6 kB	3.6 kB
		6 B	9 B	12 B	15 B	17 B
	20	4.5 kB	4.5 kB	4.5 kB	4.5 kB	4.5 kB
		7 B	10 B	14 B	17 B	20 B
	15	6 kB	6 kB	6 kB	6 kB	6 kB
		9 B	13 B	16 B	20 B	24 B
	10	9 kB	9 kB	9 kB	9 kB	9 kB
		11 B	17 B	21 B	28 B	32 B
	5	18 kB	18 kB	18 kB	18 kB	18 kB
		19 B	26 B	37 B	45 B	52 B

performance higher than 85% for all experiments beside the combination of low velocities and weak forces (see Fig. 9 for the analysis under generalized stimulation conditions). This demonstrates that the presented decoding method was efficient across a broad range of sensing conditions.

Finally, we wondered whether the decoding was able to correctly categorize stimuli independent of sensing conditions. We found that the spike train structure was consistently repeatable for the same texture across velocities once expressed in terms of the distance traveled, instead of time (Fig. 10). We defined then a sVPd that was able to decode textures across a fivefold variation of sliding velocity, with an accuracy of 90% (Fig. 12).

In addition to proper decoding performance, we are interested in evaluating how the event-based representation affects data storage, and consequently the requirements for defining a dictionary of tactile stimuli within neurorobotic applications. This objective is particularly relevant in the future perspective of achieving an artificial ability to categorize a very large set of naturalistic tactile specimens. Toward this goal, Table II shows the amount of system storage needed for both neuromorphic and raw sensor data along the sliding phase for a single sensor channel.

From this table, we can clearly appreciate the optimal storage needs of neuromorphic data in comparison to raw sensor data with the traditional constant time-sampling. A storage cost for raw sensor data depends on the number of samples (represented via their amplitude sequence), while for neuromorphic data, it depends on the number of spikes fired (represented via their timestamp sequence). Consequently, both storage costs via raw and neuromorphic data representation are affected by velocity due to the change of sliding duration to explore the 60-mm stimulus surface. Only neuromorphic data storage cost is affected by the modulation of contact force, since it correlated with firing rate (Fig. 8).

Overall, these results show the efficacy and the robustness of decoding based on neuromorphic spike trains.

B. Limits and Perspectives

The decoding algorithm accuracy was high for a set of 25 combinations of fixed forces and sliding velocities (Fig. 9). The algorithm was, however, less effective in coping with decoding across different forces than across different velocities. Still, we cannot rule out that a different decoder could be more efficient.

We used the knn decoding to classify our spike trains given the VPds between them. Bologna *et al.* [40] decoded neuromorphic mechanosensors spike trains by means of VPd, and a more complex decoding procedure called metrical information analysis [58]. Such analysis relied on the definition of a critical distance given by the maximal intrastimulus distance at the time when it becomes smaller than the minimum interstimulus distance. We preferred to use the knn classification, first, because it is more intuitive, second, because in this paper, we were not interested in the evolution over time of the decoding but only in the decoding when considering the whole spike train during sliding, and third, because we were interested in estimating the classification level in the cases in which perfect decoding was never achieved, and hence, the critical distance was not defined. In conditions in which this happens, however, the metrical information analysis provides a more robust and insightful estimate of the decoding, in particular because of the possibility to identify the exact moment in which perfect discrimination is achieved.

Other spike train decoding methods do not rely on spike train metrics. A very popular technique is the Bayesian decoding approach [59], [60], which, after convoluting the spike trains with suited kernels, computes the probability of firing in each moment associated with each stimulus and uses it to estimate the probability of each stimulus given the considered spike train. Recently, the proposed techniques also transform spike trains into continuous functions through convolution with suited kernels, and then decompose such functions using Principal Component Analysis [57] or wavelets [61] and compute mutual information between the set of the stimuli and the scores of the spike trains in the reduced space. These techniques also have several advantages, including the possibility to highlight the evolution in time of tactile information. However, decoding based on spike metrics was in our opinion a simple and effective approach to: 1) show that almost perfect decoding of naturalistic stimuli based on the neuromorphic spike trains of our device was possible and 2) highlight the relevance of spike timing for the decoding.

A limitation of the VPd-based decoding algorithm is that it was intrinsically non real-time requiring the availability of a whole window of data in order to compute the distance between trains of spikes. In addition, so far, we could not build a VPd-based decoding algorithm spanning efficiently across different forces, because the difference in timing between textures was dominated by the differences in the number of spikes across different forces for the same texture. In order to categorize textures across different forces, we built a decoder based on the combination of ISI CV and spike rate/contact force ratio. The decoding performance achieved was, however, limited to 48%. This indicates that the decoding, with the implemented modification of VPd, is more robust to velocity than to force variations. However, a more detailed study of the relation between spike rate and force, and the consequent definition of a VPd normalized both with respect to velocity and

force, could lead to an improvement of decoding efficacy, and possibly contribute to the ongoing scientific debate about the neuronal mechanisms underlying the human sense of touch.

Given the strong and reliable modulations of the activity following changes in the sensing conditions, the prior knowledge of these conditions is currently necessary to correctly perform a decoding. With the current design of the bioinspired sensor, we can estimate both quantities. The contact force can be measured from the overall spike rate prior to sliding during indentation. The transition between the two phases can be identified by the sharp change in spike rate or implementing fast adapting neuron models and detecting their activation. The sliding velocity can be estimated by the cross correlation between the responses elicited on sensors that are spatially distributed along the sliding direction [49]. A multiparametric categorization, therefore, appears to require a population code that could also be explored in neuroprosthetics through multichannel intrafascicular neural stimulation [8].

As a matter of fact, all the results presented here were based on the analysis of the neuronal output associated with a single sensor channel. The amount of information carried by the whole set of channels is at least as high, and potentially much higher, than the information carried by a single channel. Therefore, considering the spatial patterns of all channels and the temporal structure of the firing of each channel, a spatiotemporal strategy will emerge. In the planned neurorobotic experiments, this will be achieved by means of a postsynaptic layer emulating the role of the cuneate nucleus [15], [40], [41], which will also enable the real-time implementation of the stimulus decoding architecture.

ACKNOWLEDGMENT

The authors would like to thank G. Spigler, Dr. L. Beccai, and Prof. P. Dario for their previous collaboration on this project, D. Camboni and G. Kanitz for their technical support, Dr. S. Johnson for providing part of the experimented textures, Prof. H. Jörntell and Prof. J. Wessberg for explanatory conversations about the organization and coding mechanisms of the somatosensory system, and Prof. S. Micera and Prof. M. C. Carrozza for meaningful scientific discussions about translational bioengineering experiments.

REFERENCES

[1] R. F. Service, "Minds of their own," *Science*, vol. 346, no. 6206, pp. 182–183, 2014.

[2] S.-C. Liu and T. Delbruck, "Neuromorphic sensory systems," *Current Opinion Neurobiol.*, vol. 20, no. 3, pp. 288–295, 2010.

[3] G. Indiveri *et al.*, "Neuromorphic silicon neuron circuits," *Frontiers Neurosci.*, vol. 5, p. 73, May 2011.

[4] S. Mitra, S. Fusi, and G. Indiveri, "Real-time classification of complex patterns using spike-based learning in neuromorphic VLSI," *IEEE Trans. Biomed. Circuits Syst.*, vol. 3, no. 1, pp. 32–42, Feb. 2009.

[5] X. Navarro, T. B. Krueger, N. Lago, S. Micera, T. Stieglitz, and P. Dario, "A critical review of interfaces with the peripheral nervous system for the control of neuroprostheses and hybrid bionic systems," *J. Peripheral Nervous Syst.*, vol. 10, no. 3, pp. 229–258, 2005.

[6] T. Boretius *et al.*, "A transverse intrafascicular multichannel electrode (TIME) to interface with the peripheral nerve," *Biosensors Bioelectron.*, vol. 26, no. 1, pp. 62–69, 2010.

[7] R. Kwok, "Neuroprosthetics: Once more, with feeling," *Nature*, vol. 497, no. 7448, pp. 176–178, 2013.

[8] S. Raspopovic *et al.*, "Restoring natural sensory feedback in real-time bidirectional hand prostheses," *Sci. Transl. Med.*, vol. 6, no. 222, p. 222ra19, 2014.

[9] D. W. Tan, M. A. Schiefer, M. W. Keith, J. R. Anderson, J. Tyler, and D. J. Tyler, "A neural interface provides long-term stable natural touch perception," *Sci. Transl. Med.*, vol. 6, no. 257, p. 257ra138, 2014.

[10] I. Darian-Smith and L. E. Oke, "Peripheral neural representation of the spatial frequency of a grating moving across the monkey's finger pad," *J. Physiol.*, vol. 309, no. 1, pp. 117–133, 1980.

[11] Å. B. Vallbo and R. S. Johansson, "Properties of cutaneous mechanoreceptors in the human hand related to touch sensation," *Human Neurobiol.*, vol. 3, no. 1, pp. 3–14, 1984.

[12] M. Hollins and S. R. Risner, "Evidence for the duplex theory of tactile texture perception," *Perception Psychophys.*, vol. 62, no. 4, pp. 695–705, 2000.

[13] T. Yoshioka, B. Gibb, A. K. Dorsch, S. S. Hsiao, and K. O. Johnson, "Neural coding mechanisms underlying perceived roughness of finely textured surfaces," *J. Neurosci.*, vol. 21, no. 17, pp. 6905–6916, 2001.

[14] I. Birznieks, P. Jenmalm, A. W. Goodwin, and R. S. Johansson, "Encoding of direction of fingertip forces by human tactile afferents," *J. Neurosci.*, vol. 21, no. 20, pp. 8222–8237, 2001.

[15] H. Jörntell, F. Bengtsson, P. Geborek, A. Spanne, A. V. Terekhov, and V. Hayward, "Segregation of tactile input features in neurons of the cuneate nucleus," *Neuron*, vol. 83, no. 6, pp. 1444–1452, 2014.

[16] Y. Vázquez, E. Salinas, and R. Romo, "Transformation of the neural code for tactile detection from thalamus to cortex," *Proc. Nat. Acad. Sci. USA*, vol. 110, no. 28, pp. E2635–E2644, 2013.

[17] M. A. Harvey, H. P. Saal, J. F. Dammann, III, and S. J. Bensmaia, "Multiplexing stimulus information through rate and temporal codes in primate somatosensory cortex," *PLoS Biol.*, vol. 11, no. 5, pp. e1001558-1–e1001558-11, 2013.

[18] A. I. Weber *et al.*, "Spatial and temporal codes mediate the tactile perception of natural textures," *Proc. Nat. Acad. Sci. USA*, vol. 110, no. 42, pp. 17107–17112, 2013.

[19] R. S. Johansson and J. R. Flanagan, "Coding and use of tactile signals from the fingertips in object manipulation tasks," *Nature Rev. Neurosci.*, vol. 10, no. 5, pp. 345–359, 2009.

[20] G. Spigler, C. M. Oddo, and M. C. Carrozza, "Soft-neuromorphic artificial touch for applications in neuro-robotics," in *Proc. 4th IEEE RAS EMBS Int. Conf. Biomed. Robot. Biomechatronics*, Rome, Italy, Jun. 2012, pp. 1913–1918.

[21] E. M. Izhikevich, "Simple model of spiking neurons," *IEEE Trans. Neural Netw.*, vol. 14, no. 6, pp. 1569–1572, Nov. 2003.

[22] R. S. Dahiya, G. Metta, M. Valle, and G. Sandini, "Tactile sensing—From humans to humanoids," *IEEE Trans. Robot.*, vol. 26, no. 1, pp. 1–20, Feb. 2010.

[23] P. Saccomandi, E. Schena, C. M. Oddo, L. Zollo, S. Silvestri, and E. Guglielmelli, "Microfabricated tactile sensors for biomedical applications: A review," *Biosensors*, vol. 4, no. 4, pp. 422–448, 2014.

[24] C. Lucarotti, C. M. Oddo, N. Vitiello, and M. C. Carrozza, "Synthetic and bio-artificial tactile sensing: A review," *Sensors*, vol. 13, no. 2, pp. 1435–1466, 2013.

[25] A. Adamatzky, "Slime mould tactile sensor," *Sens. Actuators B, Chem.*, vol. 188, pp. 38–44, Nov. 2013.

[26] A. R. Salgarella *et al.*, "A bio-hybrid mechanotransduction system based on ciliate cells," *Microelectron. Eng.*, vol. 144, pp. 51–56, Aug. 2015.

[27] J. A. Fishel and G. E. Loeb, "Bayesian exploration for intelligent identification of textures," *Frontiers Neurorobot.*, vol. 6, p. 4, Jun. 2012.

[28] G. Vásárhelyi, M. Ádám, É. Vázsonyi, I. Bársony, and C. Dücső, "Effects of the elastic cover on tactile sensor arrays," *Sens. Actuators A, Phys.*, vol. 132, no. 1, pp. 245–251, 2006.

[29] G. Vásárhelyi, B. Fodor, and T. Roska, "Tactile sensing-processing: Interface-cover geometry and the inverse-elastic problem," *Sens. Actuators A, Phys.*, vol. 140, no. 1, pp. 8–18, Oct. 2007.

[30] J. Scheibert, S. Leurent, A. Prevost, and G. Debrégeas, "The role of fingerprints in the coding of tactile information probed with a biomimetic sensor," *Science*, vol. 323, no. 5920, pp. 1503–1506, 2009.

[31] B. Heyneman and M. R. Cutkosky, "Slip classification for dynamic tactile array sensors," *Int. J. Robot. Res.*, pp. 1–18, Mar. 2015.

[32] Y. Zhang, A. Hamilton, R. Cheung, B. Webb, P. Argyrakis, and T. Gonos, "Integration of wind sensors and analogue VLSI for an insect-inspired robot," in *Computational and Ambient Intelligence*, F. Sandoval, A. Prieto, J. Cabestany, and M. Graña, Eds. Berlin, Germany: Springer-Verlag, 2007.

[33] P. Argyrakis, A. Hamilton, B. Webb, Y. Zhang, T. Gonos, and R. Cheung, "Fabrication and characterization of a wind sensor for integration with a neuron circuit," *Microelectron. Eng.*, vol. 84, nos. 5–8, pp. 1749–1753, 2007.

[34] B. Mitchinson *et al.*, "Empirically inspired simulated electro-mechanical model of the rat mystacial follicle-sinus complex," *Proc. Roy. Soc. London B, Biol. Sci.*, vol. 271, no. 1556, pp. 2509–2516, 2004.

[35] M. Pearson *et al.*, "A hardware based implementation of a tactile sensory system for neuromorphic signal processing applications," in *Proc. IEEE Int. Conf. Acoust., Speech, Signal Process.*, Toulouse, France, May 2006, pp. 1–4.

[36] M. J. Pearson *et al.*, "Implementing spiking neural networks for real-time signal-processing and control applications: A model-validated FPGA approach," *IEEE Trans. Neural Netw.*, vol. 18, no. 5, pp. 1472–1487, Sep. 2007.

[37] T. J. Prescott, M. J. Pearson, B. Mitchinson, J. C. W. Sullivan, and A. G. Pipe, "Whisking with robots from rat vibrissae to biomimetic technology for active touch," *IEEE Robot. Autom. Mag.*, vol. 16, no. 3, pp. 42–50, Oct. 2009.

[38] J. C. Sullivan *et al.*, "Tactile discrimination using active whisker sensors," *IEEE Sensors J.*, vol. 12, no. 2, pp. 350–362, Feb. 2012.

[39] S. S. Kim, A. P. Sripati, R. J. Vogelstein, R. S. Armiger, A. F. Russell, and S. J. Bensmaia, "Conveying tactile feedback in sensorized hand neuroprostheses using a biofidelic model of mechanotransduction," *IEEE Trans. Biomed. Circuits Syst.*, vol. 3, no. 6, pp. 398–404, Dec. 2009.

[40] L. L. Bologna, J. Pinoteau, R. Brasselet, M. Maggiali, and A. Arleo, "Encoding/decoding of first and second order tactile afferents in a neurorobotic application," *J. Physiol.-Paris*, vol. 105, nos. 1–3, pp. 25–35, 2011.

[41] L. L. Bologna *et al.*, "A closed-loop neurobotic system for fine touch sensing," *J. Neural Eng.*, vol. 10, no. 4, p. 046019, 2013.

[42] W. W. Lee, J. Cabibihan, and N. V. Thakor, "Bio-mimetic strategies for tactile sensing," in *Proc. IEEE SENSORS*, Nov. 2013, pp. 1–4.

[43] W. W. Lee, H. Yu, and N. V. Thakor, "Gait event detection through neuromorphic spike sequence learning," in *Proc. 5th IEEE RAS EMBS Int. Conf. Biomed. Robot. Biomechatronics*, São Paulo, Brazil, Aug. 2014, pp. 899–904.

[44] E. K. Kim, S. A. Wellnitz, S. M. Bourdon, E. A. Lumpkin, and G. J. Gerling, "Force sensor in simulated skin and neural model mimic tactile SAI afferent spiking response to ramp and hold stimuli," *J. NeuroEng. Rehabil.*, vol. 9, no. 1, pp. 45–59, 2012.

[45] D. R. Lesniak *et al.*, "Computation identifies structural features that govern neuronal firing properties in slowly adapting touch receptors," *eLife*, vol. 3, pp. e01488-1–e01488-20, Jan. 2014.

[46] E. K. Kim *et al.*, "An engineered tactile afferent modulation platform to elicit compound sensory nerve action potentials in response to force magnitude," in *Proc. IEEE World Haptics Conf.*, Daejeon, Korea, Apr. 2013, pp. 241–246.

[47] L. Beccai *et al.*, "Design and fabrication of a hybrid silicon three-axial force sensor for biomechanical applications," *Sens. Actuators A, Phys.*, vol. 120, no. 2, pp. 370–382, 2005.

[48] C. M. Oddo, P. Valdastri, L. Beccai, S. Roccella, M. C. Carrozza, and P. Dario, "Investigation on calibration methods for multi-axis, linear and redundant force sensors," *Meas. Sci. Technol.*, vol. 18, no. 3, pp. 623–631, 2007.

[49] C. M. Oddo, M. Controzzi, L. Beccai, C. Cipriani, and M. C. Carrozza, "Roughness encoding for discrimination of surfaces in artificial active-touch," *IEEE Trans. Robot.*, vol. 27, no. 3, pp. 522–533, Jun. 2011.

[50] C. M. Oddo, L. Beccai, J. Wessberg, H. B. Wasling, F. Mattioli, and M. C. Carrozza, "Roughness encoding in human and biomimetic artificial touch: Spatiotemporal frequency modulation and structural anisotropy of fingerprints," *Sensors*, vol. 11, no. 6, pp. 5596–5615, 2011.

[51] C. M. Oddo, L. Beccai, N. Vitiello, H. B. Wasling, J. Wessberg, and M. C. Carrozza, "A mechatronic platform for human touch studies," *Mechatronics*, vol. 21, no. 3, pp. 604–613, 2011.

[52] L. A. Jones and S. J. Lederman, "Tactile sensing," in *Human Hand Function*, L. A. Jones and S. J. Lederman, Eds. New York, NY, USA: Oxford Univ. Press, 2006.

[53] E. M. Izhikevich, "Which model to use for cortical spiking neurons?" *IEEE Trans. Neural Netw.*, vol. 15, no. 5, pp. 1063–1070, Sep. 2004.

[54] N. S. Altman, "An introduction to kernel and nearest-neighbor nonparametric regression," *Amer. Statist.*, vol. 46, no. 3, pp. 175–185, 1992.

[55] R. S. Johansson and I. Birznieks, "First spikes in ensembles of human tactile afferents code complex spatial fingertip events," *Nature Neurosci.*, vol. 7, no. 2, pp. 170–177, 2004.

[56] J. D. Victor and K. P. Purpura, "Nature and precision of temporal coding in visual cortex: A metric-space analysis," *J. Neurophysiol.*, vol. 76, no. 2, pp. 1310–1326, 1996.

[57] Y. Zuo, H. Safaai, G. Notaro, A. Mazzoni, S. Panzeri, and M. E. Diamond, "Complementary contributions of spike timing and spike rate to perceptual decisions in rat S1 and S2 cortex," *Current Biol.*, vol. 25, no. 3, pp. 357–363, 2015.

[58] R. Brasselet, R. S. Johansson, and A. Arleo, "Quantifying neurotransmission reliability through metrics-based information analysis," *Neural Comput.*, vol. 23, no. 4, pp. 852–881, 2011.

[59] E. N. Brown, R. E. Kass, and P. P. Mitra, "Multiple neural spike train data analysis: State-of-the-art and future challenges," *Nature Neurosci.*, vol. 7, no. 5, pp. 456–461, 2004.

[60] I. M. Park, M. L. R. Meister, A. C. Huk, and J. W. Pillow, "Encoding and decoding in parietal cortex during sensorimotor decision-making," *Nature Neurosci.*, vol. 17, no. 10, pp. 1395–1403, 2014.

[61] V. Lopes-dos-Santos, S. Panzeri, C. Kayser, M. E. Diamond, and R. Q. Quiroga, "Extracting information in spike time patterns with wavelets and information theory," *J. Neurophysiol.*, vol. 113, no. 3, pp. 1015–1033, 2014.

Udaya Bhaskar Rongala was born in India in 1988. He received the B.Sc. degree in mechatronics engineering from SRM University, Chennai, India, in 2007, and the M.Sc. degree in European master's in advanced robotics from the Warsaw University of Technology, Warsaw, Poland, and the Ècole Centrale de Nantes, Nantes, France, in 2012. He is currently pursuing the Ph.D. degree in biorobotics with The BioRobotics Institute, Pontedera, Italy.

His current research interests include neurorobotics, cognitive robotics, tactile sensing, and neural coding.

Alberto Mazzoni was born in Florence, Italy in 1978. He received the Laurea (*magna cum laude*) degree in theoretical physics from the University of Pisa, Pisa, Italy, in 2002, and the Ph.D. degree in neurobiology from the International School for Advanced Studies, Trieste, Italy, in 2007.

From 2007 to 2009, he was part of the Theoretical Neuroscience Group with the Institute for Scientific Interchange. From 2009 to 2013, he was part of the Neural Coding Group with the Fondazione Istituto Italiano di Tecnologia. Since 2014, he has been with The BioRobotics Institute, Scuola Superiore Sant'Anna, Pontedera, Italy. His aim is to foster the integration of computational neuroscience and neuroengineering. He has authored papers ranging from invertebrate motor control to primate vision, all in a computational neuroscience perspective. His current research interests include the study of neural processing of sensory stimuli and motor commands by means of information theory and decoding theory tools, and the development of in-silico modeling of neuronal networks.

Calogero Maria Oddo (M'14) received the B.Sc. and M.Sc. (Hons.) degrees in electronics engineering from the University of Pisa, Pisa, Italy, and the First and Second level (Hons.) degrees in industrial and information engineering and the Ph.D. (Hons.) degree in biorobotics from Scuola Superiore Sant'Anna (SSSA), Pisa.

He is currently an Assistant Professor of BioRobotics and the Head of the Human Machine Nexus Laboratory with The BioRobotics Institute, SSSA, supervising a team of 11 research fellows. He has authored over 40 conference and journal publications with a focus on integrating robotics and neuroscience. At SSSA, he holds courses on FPGA logics and neuromorphic engineering for undergraduate and Ph.D. students. He is the scientific responsible of the biorobotics section of the second level master on digital life and smart living activated at SSSA in collaboration with TIM - Telecom Italia company, Rome, Italy.